

CHAPTER 2

Theory

In this Chapter, theories of aerosol particle, particle properties, creating charged particles and measuring by electrical method, including statistics for comparing a measuring data, and numerical models are described and presented. First Section of the Chapter describes the definition of PM including size, shape, and density, and considers the other particle theory that are needed to classify the particle size. The second Section describes briefly a diffusion drying principle to decrease the humidity in the air. Electrical properties in the Section 3 is needed to validate the particle charging mechanism in Section 4. In addition, filter and deposition mechanism, measurement of flow rate and net charge concentration, and data acquisition in Section 5, 6, and 7, respectively, which needed for processing accurate data. Section 8 shows a requirement for data acquisition that can obtain an accurate data. Section 9 shows a guideline for comparing the detector with standard detectors and need for statistic theory, shown in Section 10. Finally, the numerical theory needed for validating the component designed that used in Chapter 3 and 4, respectively.

2.1 Properties of PM

2.1.1 Definition. Aerosol refers to the solid particles and the liquid droplets suspended in the air. Particles that spread in the air a large and visible as black as soot and smoke, but some type are so small and is not visible to the naked eye. Aerosols are typically less than 100 μm in diameter. Dust can affect the health of people, animals, plants, and was damage to buildings, causing a nuisance to the public, obscured vision, causing difficulties in communication and transportation. Many countries have established standards for the aerosol particle in the air ambient. Airborne PM or aerosol is defined as solid, liquid or a combination of both suspended in gas or air with a diameter in the range of 1 nm to 100 μm . Particle size is generally the key variable that explains behavior, chemical composition and physical properties of aerosol particles. In general,

the particles will separate by the size and speed of precipitation. Particles that are larger than 100 μm in diameter are precipitated faster (between seconds to minutes). The particles smaller than 1 μm in diameter precipitate slowly to very slow, (between hours to days), sometimes considered to be floating in the air permanently. The classification of aerosols is based on the shape and diameter as follows (Hinds 1999; Intra *et al.* 2016).

Smoke is particles of carbon that combines with particles of liquid that comes from incomplete combustion. Generally, it have 0.1 to 1 μm in diameter range. It is spherical for fluid and not a uniform shape for solid, the smoke that small is a long time for suspensions and motion and moving with random motion. Dust is a small solid particles in the air with a diameter ranging from 1 μm to 200 μm or bigger. Dust particles have no definite shape and the size is an average of each particle different. Vapor or mist is particles caused by condensation or sublimation, it is very slow precipitate and have a motion by Brownian type and have 0.1 to 1 μm in diameter range. Fog (smog) have 2 to 200 μm in diameter range, while water droplets are larger than 200 μm was held in category of raindrops. Total Suspended Particulate (TSP) or PM100 in general atmosphere, it means particle matter that less than 100 μm diameter. PM10 in general atmosphere, it means PM that less than 10 μm in diameter. PM2.5 in general atmosphere, it means PM that less than 2.5 μm in diameter. PM1.0 in general atmosphere, it means PM that less than 1.0 μm in diameter (Hinds 1999; Intra *et al.* 2016).

2.1.2 Particle Size, Shape, and Density. Particle size is the most important parameter for characterizing the behavior of aerosol. All properties of aerosol depend on particle size strongly. In addition, most aerosols cover a wide range of sizes. A hundredfold range between the smallest and largest particles of an aerosol is common. Furthermore, the nature of the laws governing these properties may change with particle size. The yardstick or prefix unit of particle size is the micrometer (μm) or micron (μ), which is 10^{-6} m and the particle diameter is given the symbol d_p . Figure 2.1 shows size ranges for aerosols and other phenomena. This picture covers a size range of 10^7 from gas molecules to a millimeter-sized particle. In general, the particle sizes range from 0.01 to 100 μm are dusts, ground material, and pollen. This particle is in the micrometer range or larger, while fumes and smokes are sub-micrometer. The smallest aerosol particles approach the size of large gas molecules and have many of their properties. Ultrafine particles or

nanoparticles cover the range from large gas molecules to about 100 nm (0.001 to 0.1 μm). Particles greater than 10 μm has limited stability in the atmosphere, but still can be an important source of occupational exposure because of a worker's proximity to the source. The largest aerosol particles are visible grains that have the properties described by the familiar Newtonian physics of baseballs and automobiles. The dots letter has a diameter of about 400 μm , while the smallest grains of flour that one can see under normal condition are 50-100 μm . The finest wire mesh sieves have openings of about 20 μm . The wavelength of visible is in the sub-micrometer size range about 0.5 μm . Liquid aerosol particles are nearly always spherical, while solid aerosol particle are several shapes. In the development of the theory of aerosol properties, it is usually necessary to assume that the particles are spherical. An equivalent diameter is the diameter of the sphere that has the same value of a particular physical property as that of an irregular particle. The physical property of interest is the particle density (kg/m^3). Particle density refers to the mass per unit volume of the particle itself, and this density called concentration. Liquid particles and crushed or ground solid particles have a density equal to that of their parent material. Smoke and fume particles may have apparent densities significantly less than that predicted from their chemical composition. Standard density is determinate by the density of water at about 1,000 kg/m^3 , while the density of air is 1.20 kg/m^3 (Hinds 1999).

2.1.3 Source of Aerosol Particle. Generally, aerosol particle are generated from natural and man-made sources, such as forest fires, airborne sea salt, windblown dust, and haze in the Smoky Mountain, smoke from power plants, agricultural burning, particles in automotive exhaust, and test aerosols generated in a laboratory. The dust that smaller than 0.1 μm in diameter is generated from vehicle exhaust, reactions between various gases, smoke, dust storms, sea spray and industry. Dust between 0.01 to 1.0 μm in diameter is generated from a combination of smoke, exhaust steam. Dust between 0.4 to 0.9 μm in diameter is generated in light distribution and dusky sky. Dust that larger than 1.0 μm in diameter was generated from a combination of more smoke, ash, powders of attrition, pollen and insects. Typical aerosols are composed of particles with different sizes. The monodisperse aerosol type consists of the same size particles and can be created in the laboratory and used for testing. However, aerosols are typically polydisperse, a wide range of particle sizes. Typically, the aerosol size distribution is lognormal. Distribution

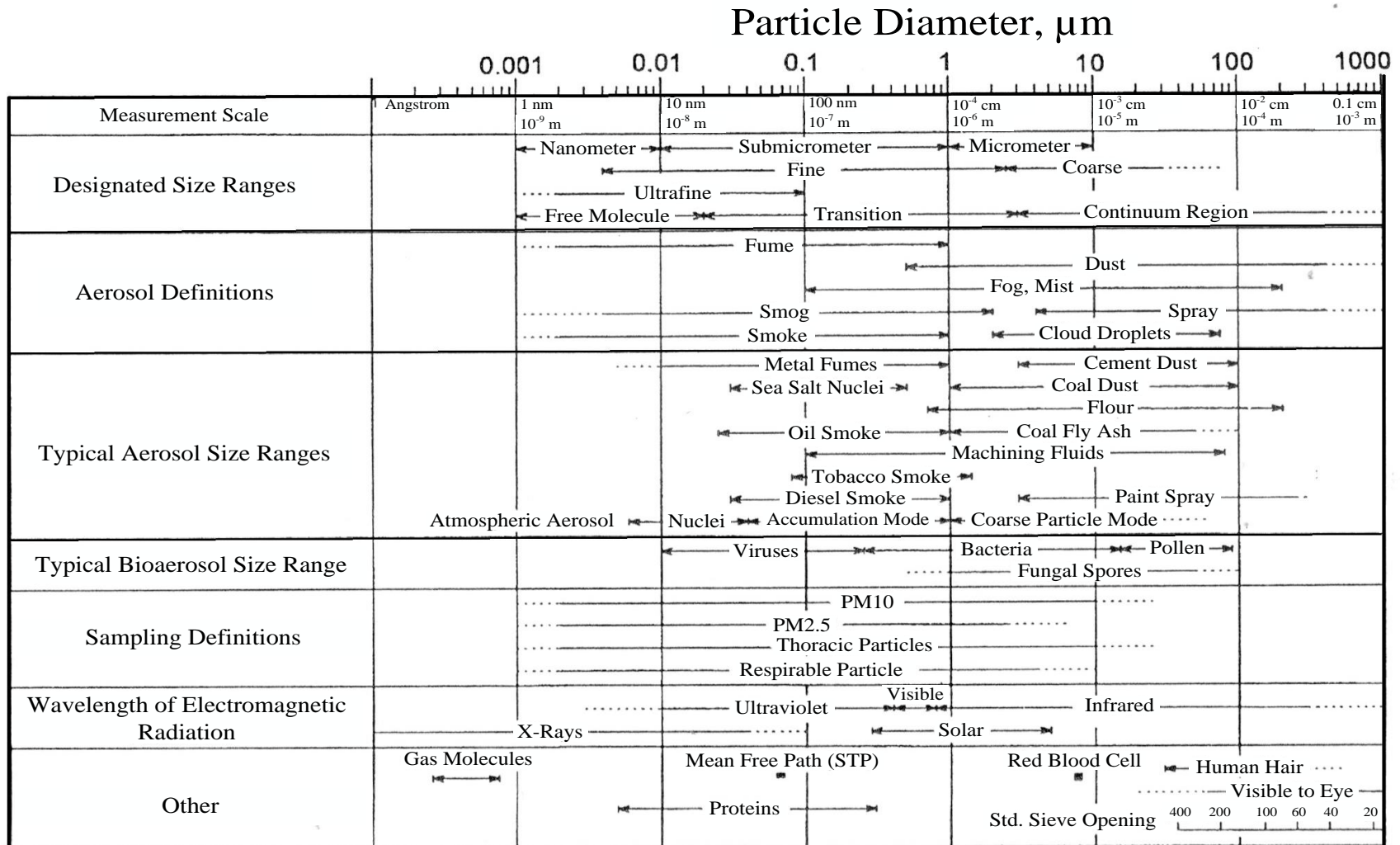


Figure 2.1 Particle size ranges and definitions for aerosol (Hinds 1999).

function can be divided into three main modes that are nuclei mode, accumulation mode and coarse mode, as shown in Figure 2.2. The particle is separated by the size of dust in the air, between 1 nm to 100 μm in diameter. Nuclei mode (include with Aitken mode) particles consist of particles less than 100 nm in diameter. This particle mode is created from the origin and mold caused by the gas-to-particle conversion and the condensation processes. In this mode, the particles have a number weighted size distribution of the particles that are small and have very little mass. Accumulation mode particles have a size range between about 100 nm and 1 μm in diameter, such as products from organic materials, smoke particles, particles from burning or combustion particles and the nuclei mode particle that together with the accumulation mode. The particles in this mode are created by sticking together of particles in the mode nuclei, thus have a greater size but a lesser amount. So there is distributed by a mass weighted particle size. Coarse mode particles consist of particles that larger than 1 μm in diameter, such as dust, particles of sea-salt. Particles are from machinery, such as agriculture and mines, although the coarse mode particles have big mass, but these particles are in very small numbers, if compared to the accumulation and nuclei mode particles (Hinds 1999; Intra *et al.* 2016).

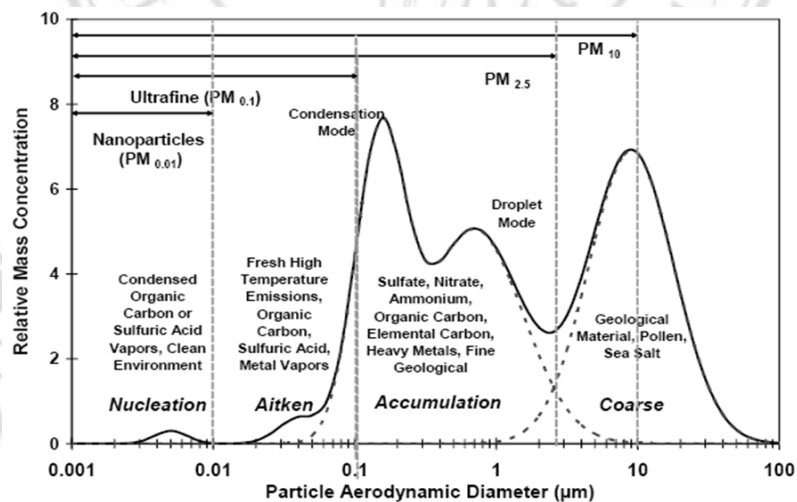


Figure 2.2 The size distribution of dust aerosols (Theophanides *et al.* 2011).

2.1.4 Aerosol Concentration. The most important and most commonly measured aerosol property for measuring health and environmental effect is the mass concentration, which is the mass of PM in a volume of aerosol (g/m^3 , mg/m^3 , or $\mu\text{g}/\text{m}^3$). The mass concentration is equivalent to the density (ρ) of the ensemble of aerosol particle in the air. Another common measurement of concentration is the number concentration which

is the number of particles per unit volume of aerosol (particle number/m³), this unit popularly used for the measurement of bio-aerosol and fibers. An older unit is million particles per cubic foot or “mppcf”. A both concentration unit is different with gaseous contaminants as a volume ratio or mass ratio in parts per million (ppm) which not used for aerosols measurement. Because of aerosol concentration is numerically very low when expressed in ppm unit (Hinds 1999).

2.1.5 Standard of the Airborne PM. Many organizations use different air pollution standards such as Air Quality Health Index (AQHI from Canada), Air Pollution Index (API from Hong Kong), Indice Metropolitano de la Calidad del Aire (IMECA from Mexico), Pollutant Standards Index (PSI from Singapore), Comprehensive Air-quality Index (CAI from South Korea), Committee On Medical Effects of Air Pollutants (COMEAP from United Kingdom), Common Air Quality Index (CAQI from Europe), Air Quality Index (AQI from United States). Thailand and Asian countries use AQI standard according to United States. Although, several countries have different report methods, but all of pollution indices are calculated from PM which shows that it is an important variable for air pollution. Pollution control department (PCD) of Thailand uses the AQI in reporting the air pollution (AQI 2016).

The United States recognizes importance of the problem of air pollution. United State Environmental Protection Agency (US EPA) is an agency of the United States that is responsible for protecting the health of humanity and protecting the natural environment, including an air, soil and water. US EPA has set a standard of “Total Suspended Particulate (TSP) or PM100 on 1971, but research found that the small size particle is more dangerous than TSP, which can pass to deep of the respiratory system so US EPA rejected TSP standard and set new PM standard on PM10 and PM2.5 in 1987 and 1997, respectively. Then the federal government of the United States has imposed Code of Federal Regulations (CFR) up to 50 items by the part 50 is the national primary and secondary ambient air quality standards. It is in Subchapters C of air programs in “Chapter I Environmental Protection Agency” under Title 40 Protection of Environment, respectively, which this international standards have been deployed around the world. PM10 in US EPA means the coarse particle or particle that smaller than 10 µm diameter generated from traffic, materials transport on the road, dust from crushing and PM2.5 is

fine particles that smaller than 2.5 μm diameter generated from exhaust engine, power plant, industrial, dust from firewood burning. PM10 and PM2.5 standard of CFR specified in part 50 for “National Primary and Secondary Ambient Air Quality Standard” or NAAQS. The guide line standard of the PM is shown in Table 2.1. While, PM1.0 standard and guideline are not specified in many organizations which could be used soon (US EPA 2016; CFR 2016; WHO 2016; PCD 2016; EPA 2016).

Table 2.1 The guideline standard of PM (EPA 2016; PCD 2016; WHO 2016).

Average of PM standard	TSP		PM10		PM2.5	
	24 h	1 y	24 h	1 y	24 h	1 y
Primary-NAAQS (1971)	260	75	n/a	n/a	n/a	n/a
Secondary-NAAQS (1971)	150	60	n/a	n/a	n/a	n/a
Primary and Secondary NAAQS (1987)	150	60	150	50	n/a	n/a
Primary and Secondary NAAQS (1997)	150	60	150	50	65	15
Primary and Secondary NAAQS (2006)	150	60	150	50	35	15
Primary-NAAQS (2013)	150	60	150	50	35	12
Secondary-NAAQS (2013)	150	60	150	50	35	15
Primary and Secondary NAAQS (2013)	150	60	150	50	35	15
Appendix N of CFR Part 50 (2015)	150	60	150	50	65	15
World Health Organization; WHO (2005)	230	90	50	20	25	10
Thailand (2010)	330	100	120	50	50	25

2.1.6 Properties of Gases and Important Concerned Variable. Newton's law of viscosity gives the frictional force between fluid layers moving at different velocities. Consider two parallel plates as shown in Figure 2.3 where the area (A) separated by a distance (y) that is small compared with the dimensions of the plates. One plate moves with a constant velocity (U), while the other is stationary. The gas (or liquid) between the plates resists the motion, so a force (F) has to be continuously applied to maintain a constant velocity. This force is proportional to the area of the plates and to the relative velocity of one plate with respect to the other and is inversely proportional to the distance between the plates as shown in Eqs. (2.1) where η is the proportionality constant called the coefficient of dynamic viscosity or the viscosity. It has several units in SI unit as $\text{N}\cdot\text{s}/\text{m}^2$, $\text{kg}/\text{m}\cdot\text{s}$, or $\text{Pa}\cdot\text{s}$. The viscosity of air at standard temperature (20°C) is 1.81×10^{-5} $\text{Pa}\cdot\text{s}$ (Hinds 1999). The viscosity of a gas is independent of pressure, but it should increase with temperature as shown in Eqs. (2.2) and Figure 2.4, where η_r and T_r is the viscosity and temperature of a gas at standard condition, respectively. In addition, the viscosity is

depended on the Sutherland interpolation constant (S) as shown in Eqs. (2.3) (Willeke and Baron 1993).

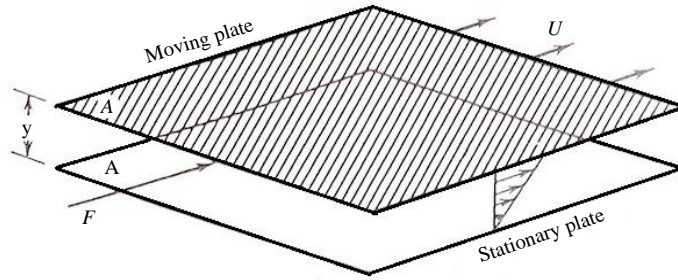


Figure 2.3 Fluid resistance between two parallel plates (Hinds 1999).

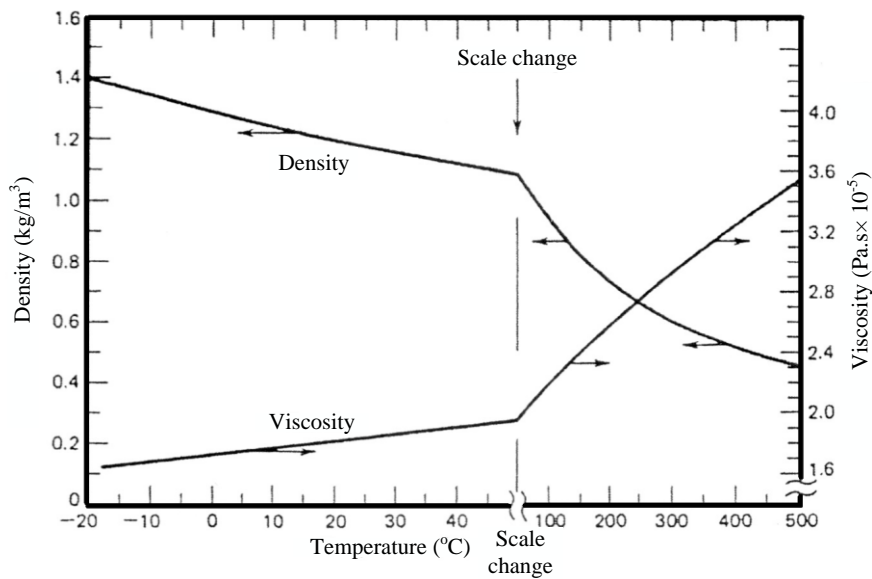


Figure 2.4 Density and viscosity of air versus temperature (Hinds 1999).

Reynold number (Re) as shown in Eqs. (2.4) is an index number indicated that flow effect of fluid which is related to inertia force and velocity force. Eqs. (2.5) is calculated the Particle Reynold number (Re_p) which it used to apply validations to flow in the pipe or the particle motion. Fluid flow around a sphere particle can be validated from this Reynold number, it is laminar flow type at $Re < 1$, and turbulent flow type at $Re > 1$ as shown in Figure 2.5 (Hinds 1999).

$$F = \frac{\eta AU}{y} \quad (2.1)$$

$$\frac{\eta}{\eta_r} = \left(\frac{T}{T_r} \right)^{0.74} \quad (2.2)$$

$$\eta = \eta_r \left(\frac{T_r + S}{T + S} \right) \left(\frac{T}{T_r} \right) \quad (2.3)$$

$$Re = \frac{\rho VD}{\eta} \quad (2.4)$$

$$Re_p = \frac{\rho V_p d_p}{\eta} \quad (2.5)$$

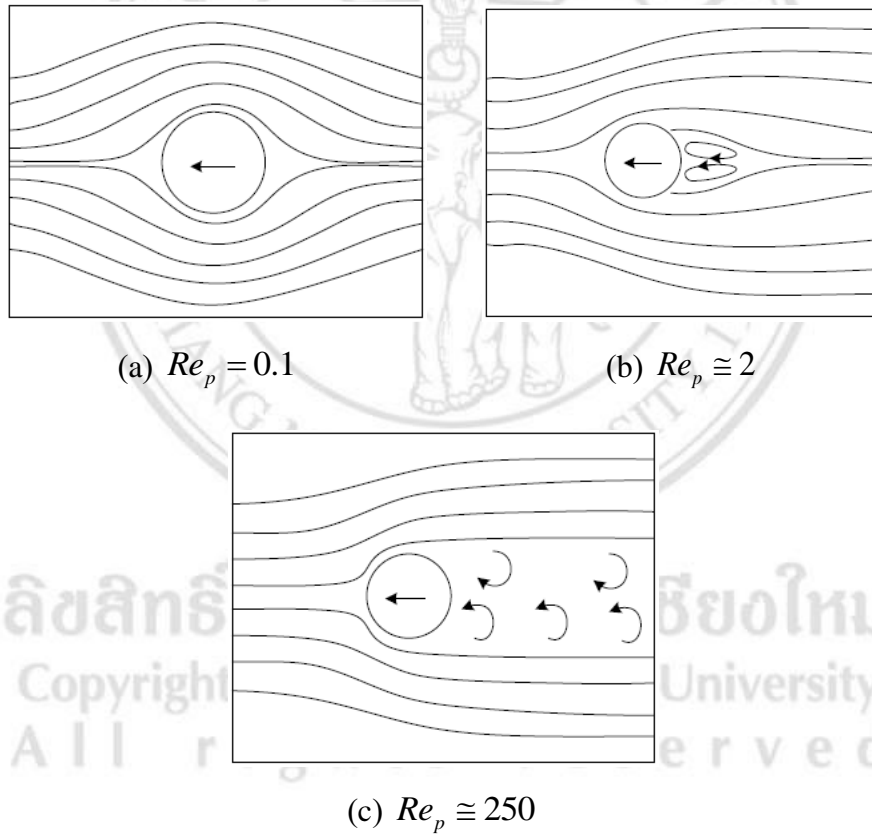


Figure 2.5 Fluid flow around the spherical particle (Hinds 1999).

When a spherical particle has a rapid move in gas, it has the gas resistance force or drag force (F_D). Newton's Resistance Equation or Newton's law is valid for a wide range of particle motion, but is useful primarily of Reynolds numbers greater than 1,000 that not to aerosol particle (such as a cannonball). General form of Newton's Resistance

Equation is shown in Eqs. (2.6) where C_D is the coefficient of drag, ρ_g is the gas density, d_p is the particle diameter, and V is the particle velocity. For the Reynold number less than 1, Stokes's Law is appropriate for study the aerosol. The general form of Stokes's Equation is shown in Eqs. (2.7), which it contains viscosity, but not associated with the inertia, while Newton's law contains the inertia. Comparing between Stokes's Law and Newton's law as shown in Eqs. (2.8), it was found that can solve and given in Eqs. (2.9) (Hinds 1999).

$$F_D = C_D \frac{\pi}{8} \rho_g d_p V^2, \text{ Newton's law} \quad (2.6)$$

$$F_D = 3\pi\eta d_p V, \text{ Stokes's law} \quad (2.7)$$

$$F_D = 3\pi\eta d_p V = C_D \frac{\pi}{8} \rho_g d_p V^2, \text{ for } Re < 1 \quad (2.8)$$

$$C_D = \frac{24\eta}{\rho_g d_p V} = \frac{24}{Re} \quad (2.9)$$

Stokes's law used for determining the velocity of an aerosol particle undergoing gravitational settling in still air. When a particle is released in air, it was settling with velocity. The drag force of the air on the particle (F_D) is exactly equal and opposite to the gravity force F_G ($F_D = F_G$) and it is proportional to the particle mass concentration (m_p) and the gravitational acceleration (g) as shown in Eqs. (2.10), where the particle mass concentration is a relationship between the particle volume (v_p) and the particle density (ρ_p), the gravitational force can be write in Eqs. (2.11). The terminal settling velocity (V_{TS}) is calculated from the drag force and the gravity force as shown in Eqs. (2.12) where ρ_p is the density of the particle, g is the acceleration of gravity. In addition, the particle mobility (B) can be measured from the relative each of producing steady motion for an aerosol particle as shown in Eqs. (2.13), it has units of m/N.s and is often called mechanical mobility, which differ from electrical mobility. In addition, the terminal settling velocity can be found from the particle mobility and the drag force as shown in Eqs. (2.14) (Hinds 1999).

$$F_D = F_G = m_p g = \rho_p v_p g = \left(\frac{\pi d_p^3}{6}\right) \rho_p g \quad (2.10)$$

$$F_G = \frac{\pi}{6} d_p^3 \rho_p g \quad (2.11)$$

$$V_{TS} = \frac{\rho_p d^2 g}{18\eta}, \text{ for } d > 1 \mu\text{m and } Re < 1 \quad (2.12)$$

$$B = \frac{V}{F_D} = \frac{1}{3\pi\eta d}, \text{ for } d > 1 \mu\text{m} \quad (2.13)$$

$$V_{TS} = F_G B \quad (2.14)$$

For particle less than 1 μm , the particle mobility must be multiplied by the slip corrector factor. In 1910, Cunningham derives a correction factor for Stokes's law, the factor called the Cunningham correction factor (C_c) and getting Eqs. (2.15) for the particle less than 1 μm . The mean free path (λ) can be calculated from Eqs. (2.16) where d_m is the collision diameter of the molecule. The mean free path of air at standard condition is 0.066 μm (Hinds 1999), while it depends on the temperature and pressure as shown in Eqs. (2.17), where P_r is the pressure at standard temperature (Willeke and Baron 1993). In addition, the Cunningham correction factor still depends on the pressure as shown in Eqs. (2.18) and has a difference in various particle sizes as shown in Figure 2.6 (Hinds 1999).

$$C_c = 1 + \frac{\lambda}{d} \left(2.34 + 1.05 \exp\left(-0.39 \frac{d}{\lambda}\right) \right) \quad (2.15)$$

$$\lambda = \frac{1}{\sqrt{2} n \pi d_m^2} \quad (2.16)$$

$$\lambda = \lambda_r \left(\frac{P_r}{P} \right) \left(\frac{T}{T_r} \right) \left(\frac{1 + S/T_r}{1 + S/T} \right) \quad (2.17)$$

$$C_c = 1 + \frac{1}{Pd} (15.60 + 7.00 \exp(-0.059Pd)) \quad (2.18)$$

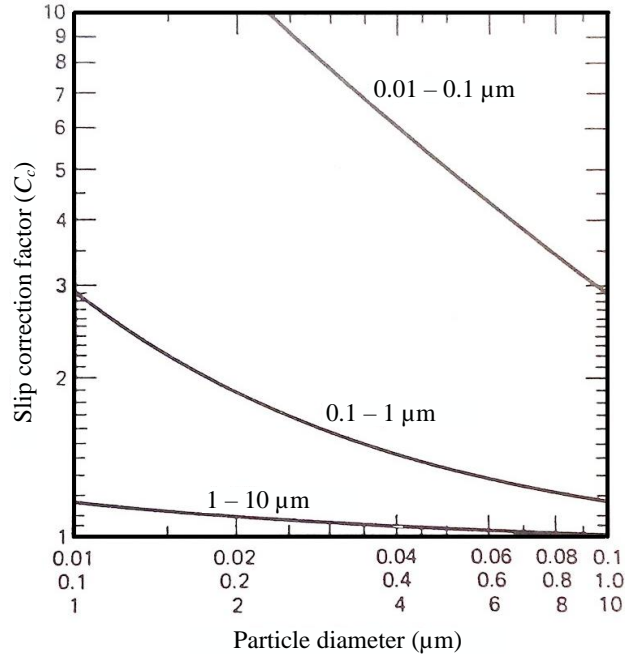


Figure 2.6 Slip correction factor at 20 °C and 101 kPa (Hinds 1999).

The dynamic shape factor (χ) used is a correction factor for non-spherical particle. The dynamic shape factor of the spherical particle equal 1, while the non-spherical particle has more than 1 such as a quartz is 1.36, cube is 1.08, and talc is 1.88 etc. A liquid droplets (less than 1 nm) and some solid particle formed by condensation are spherical, while most other types of particles are non-spherical. The dynamic shape factor can be calculated from Eqs. (2.19) where d_e is the equivalent volume diameter, it is the diameter of a sphere having the same volume as the irregular particle. Finally, the application form of the drag force and the terminal settling velocity at ($F_D = F_G$) in Stokes' s region are shown in Eqs. (2.20) and (2.21), respectively (Hinds 1999). Particle motion in an electric field called electrophoresis, this condition the electrostatic forces (F_E) can be estimated from Eqs. (2.22) where n is the number of charge, e is the elementary unit of charge (1.6×10^{-19} Coulomb), E is the electric field. This electrostatic force can effect on the particle motion and can be calculated the terminal velocity (V_{TE}) from Eqs. (2.23) (Willeke and Baron 1993).

$$\chi = \frac{F_D}{3\pi\eta V d_e} \quad (2.19)$$

$$F_D = \frac{3\pi\eta d_p V \chi}{C_c} \quad (2.20)$$

$$V_{TS} = \frac{\rho_p d_p^2 g C_c}{18\eta\chi} \quad (2.21)$$

$$F_E = neE \quad (2.22)$$

$$V_{TE} = \frac{neEC_c}{3\pi\eta d_p} \quad (2.23)$$

2.1.7 Aerodynamic Diameter and Stokes' s Diameter. Due to the fact that several particles are non-spherical, so the equivalent diameter (d_e) is used to estimate the particle diameter (d_p). Aerodynamic diameter (d_a) is defined from the same movement, but Stoke diameter (d_s) is defined from the same density. Consider Figure 2.7, the irregular particle of quartz, the spherical particle ($d_p = 4.3 \mu\text{m}$), and the spheres of water droplet ($d_p = 8.6 \mu\text{m}$) are falling to the ground with the same settling velocity of 2.2 mm/s. When release the irregular particle (Figure 2.7a) ($d_e = 5.0 \mu\text{m}$) together with the spherical particle (Figure 2.7c) which has 1,000 kg/m³ in density (the density of water droplets) then both falling to the ground simultaneously at $V_{TS} = 2.2 \text{ mm/s}$, both have aerodynamic diameter properties that $d_a = 8.6 \mu\text{m}$. While, the spherical particle (Figure 2.7b) has the particle density same the irregular particle (Figure 2.7a) at 4,000 kg/m³, the irregular particle has d_s equal 4.3 μm . V_{TS} in this case getting from Eqs. (2.24) where ρ_p is the particle density, ρ_0 is the standard particle density (1,000 kg/m³ from the water droplet), ρ_b is the normal density of the bulk material of the particle (Hinds 1999).

2.1.8 Particle Motion. Particle motion is important for describing the aerosol collection mechanisms that operate in a fibrous filter and the impactor. Three variables that used for analysis the motion, are the relaxation time, stopping distance, and Stokes number. The relaxation time (τ) is a quantity from the relation of the particle mass and mobility (mB), this time was depended on the particle diameter (d) as shown in Eqs. (2.25). The relaxation time is restricted to particle motion in the Stokes region, where

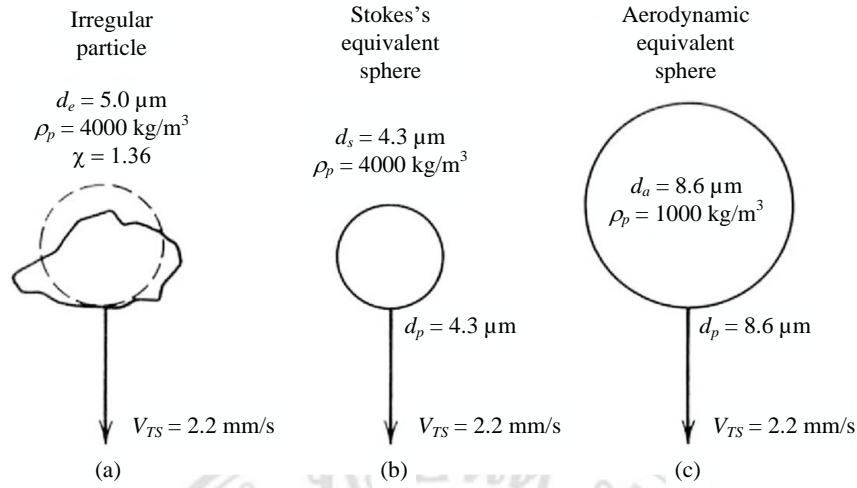


Figure 2.7 An irregular particle and its equivalent spheres (Hinds 1999).

$Re < 1$. The stopping distance (S) represents a measure of a particle's effective initial momentum, which is decreased to zero by air friction over a distance equal to the stopping distance. The stopping distance as shown in Eqs. (2.26) is accurate only in the Stokes region or the Reynold number of the particle at the initial velocity (Re_0) (Eqs. 2.27) less than 1.0, while Eqs. (2.28) used for calculating the stopping distance at $1 < Re_0 < 400$ region.

$$V_{TS} = \frac{\rho_p d_e^2 g C_c}{18\eta\chi} = \frac{\rho_p d_s^2 g C_c}{18\eta} = \frac{\rho_0 d_a^2 g C_c}{18\eta} \quad (2.24)$$

$$\tau = mB = \rho_p \frac{\pi}{6} d^3 \left(\frac{C_c}{3\pi\eta d} \right) = \frac{\rho_p d^2 C_c}{18\eta} = \frac{\rho_0 d_a^2 C_c}{18\eta} \quad (2.25)$$

$$S = \tau V_0 = \frac{\rho_0 d_a^2 C_c}{18\eta} V_0 \quad (2.26)$$

$$Re_0 = \frac{\rho_s}{\eta} V_0 d \quad (2.27)$$

$$S = \frac{\rho_p d}{\rho_s} \left[Re_0^{1/3} - \sqrt{6} \arctan \left(\frac{Re_0^{1/3}}{\sqrt{6}} \right) \right] \quad (2.28)$$

When particle is injected horizontally in the air, curvilinear motion is one of the trajectory movement behavioral. This motion is characterized by a dimensionless number called the Stokes number (Stk). For example, the fluid flow in a cylindrical pipe and a perpendicular plate, the Stokes number is the ratio of the stopping distance and a diameter of cylinder diameter (d_c) as shown in Eqs. (2.29), in case $Re_0 < 1.0$, the stopping distance getting from Eqs. (2.26), but $Re_0 > 1.0$, the stopping distance getting from Eqs. (2.28). In addition, Stoke number is the parameter that governs the collection efficiency of the inertial impactor. Stoke number of a simple impactor as shown in Figure 2.8 is calculated from Eqs. (2.30), which the jet radius ($D_j / 2$) considering substitute. All particles greater than an aerodynamic size are collected, while all particles less than that size pass through. This aerodynamic size is called the cutoff size, cutoff diameter, cut point, cut-size, cut off, or d_{50} . As a practical matter, most well-designed impactors can be assumed to be ideal and their efficiency curves are characterized by a single number Stk_{50} , the Stoke number that gives 50% collection efficiency. Ideal cutoff curve as shown in Figure 2.9 is the aim of the impactor design, but it accepted at 50% efficiency by a single number Stk_{50} mean the Stokes number that gives 50% collection efficiency. The actual cutoff curve is assumed that the mass of particle larger than the cutoff size that through (the upper shaded area) equals the mass of particles below the cutoff size that are collected (the lower shaded area). Stokes number equations can be rearranged to give the particle diameter having 50% collection efficiency (d_{50}) where the velocity (V) comes from the particle flow rate (Q) as shown in Eqs. (2.31). This equation is in terms of the Cunningham correction factor (C_c) which it can find d_{50} from Eqs. (2.32) in μm unit (Hinds 1999).

$$Stk = \frac{S}{d_c} = \frac{\tau V_0}{d_c} \quad (2.29)$$

$$Stk = \frac{\tau V_0}{D_j / 2} = \frac{\rho_p d_p^2 V C_c}{9\eta D_j} \quad (2.30)$$

$$d_{50} \sqrt{C_c} = \left[\frac{9\pi\eta D_j^3 (Stk_{50})}{4\rho_p Q} \right]^{1/2} \quad (2.31)$$

$$d_{50} = d_{50} \sqrt{C_c} - 0.078 \quad (2.32)$$

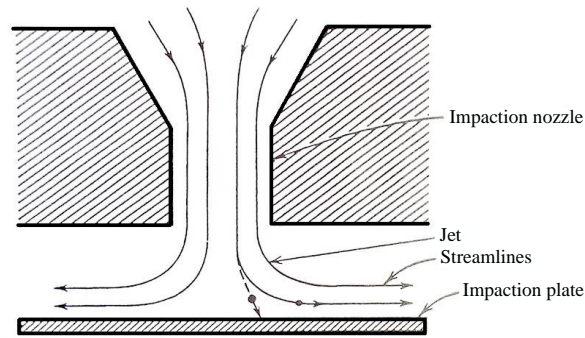


Figure 2.8 Cross-sectional view of an impactor (Hinds 1999).

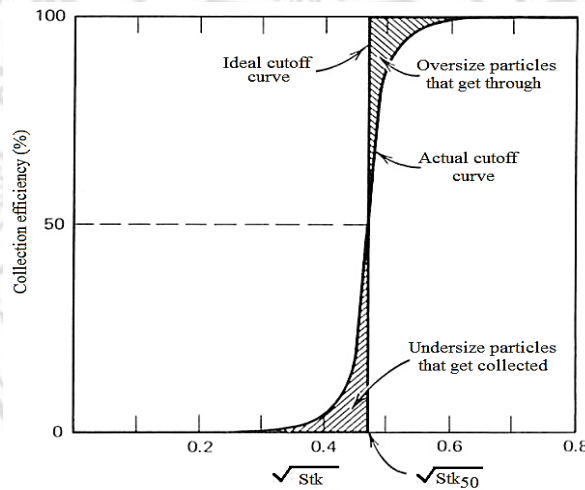


Figure 2.9 The collection efficiency and cutoff curve between actual and idea impactor (Hinds 1999).

2.1.9 Particle Size Classification. There are many particle classification methods, depending on diameter as shown in Figure 2. 10. For example, the transmission electron microscope (TEM) and the scanning electron microscope (SEM) are suitable for 0.01 – 10 μm diameter, however the inertial or impactor method is suitable for 0.1 – 50 μm diameter. The inertial method is recognized internationally for classifying the particle. This method is used to classify the particles in reference and equivalent method as required for measuring the airborne PM of US EPA. This method uses inertial mechanism principle that the particles flow out of the streamline, due to the fact that particles have a mass that cannot follow the main cave and the impaction plate collects this particle (Hinds 1999).

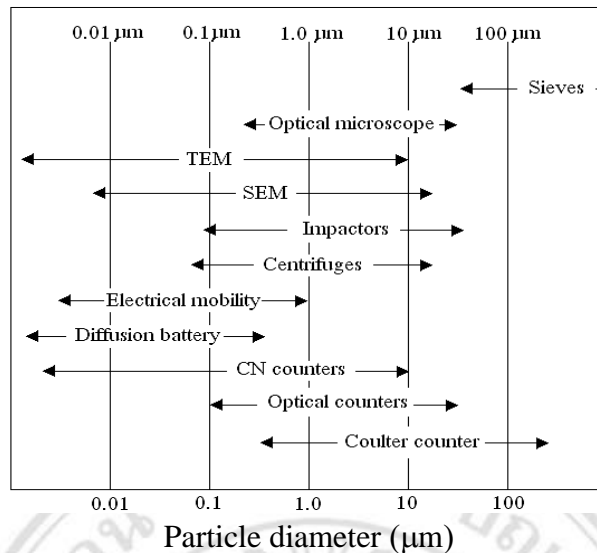


Figure 2.10 Particle classification method in diameter size range (Hinds 1999).

2.2 Diffusion Drying

Hygroscopic of the filter media and particles is associated with error to the continuous PM monitor, the RH is needed to be removed from the air sample. The RH can decrease by decreasing the ambient temperature down to under the dew point temperature. This method makes the air condense to water which is popular for high volume air in industry. A heat exchange principle used for making an air temperature lower than the dew point then the air will condense into water droplets. When the RH in the air turn into the water droplet, it can be absorbed by the silica gel. This technique is appropriate for more than 4 L/min in flow rate and can remove the RH up to 50% from the inlet. The mass of silica gel (Q_{kg} in kilogram) can be calculate from Eqs. (2.32) where C_{eq} is the concentration of water vapor at saturation, D is the difference humidity between inner and outer, V is the volume of the diffusion chamber, N is the number of air exchanges per day, t is the maximum date that accepted, M_H is the hysteresis corrected buffering capacity of silica gel, F is the acceptable maximum range of RH fluctuation (Steven 2002). Nafion® is a RH absorbing device by heat exchange under dew point temperature. The samples air will collide the cool air inside the Nafion, then the dry air particle can pass through the air outlet (Motupally *et al.* 2000). This method is appropriate with low flow rate samples, such as TEOM instrument (Meyer *et al.* 2011). The diffusion absorbing method is a popular method for removing the RH from the air

samples. The absorbing material may be charcoal, activated carbon, or silica gel. Silica gel is a silicon dioxide that has an extremely porous structure (about 2.4 nm in average diameter). Silica gel is a desiccant that has a spherical shape (about 2-5 mm in diameter) in white, blue or orange types which a color change when it absorbing a humidity. It can absorb vapors and there is no change in the size or shape of them when saturated. It can be reused after baking for removal a humidity (about 180 °C in 2 h). Generally, a silica gel has an absorption capacity for water vapor at less %RH ambient, but this capacity has increased at high %RH ambient. (Farnsworth 2009; Lassen 1953; Tuch *et al.* 2009).

$$Q_{kg} = \frac{(C_{eq} D) V (Nt)}{M_H F} \quad (2.32)$$

2.3 Electrical Properties

Coulomb's law is the fundamental equation of electrostatics, which gives the electrostatic force (F_E) between two point charges (q and q') that have a distance (R) as shown in Eqs. (2.33), where q is the amount of charge, K_E is the constant of proportionality that depends on the system of unit used. Ampere (A) is one of the seven SI base units, it is defined as the current required to produce a specified force between two parallel wires 1 m apart. Coulomb (C) is a unit of charge. It is defined as the amount of charge transported in 1 s by a current of 1 A. Volt (V) is a potential difference between two points along a wire carrying 1 A. Watt (W) is a dissipating of power between the points. In SI unit, K_E is evaluated from Eqs. (2.34) where ϵ_0 is the permittivity of the vacuum ($8.85 \times 10^{-12} \text{ C}^2/\text{N.m}^2$). F_E can be calculated again in Eqs. (3.35) (Hinds 1999).

An electric field strength or intensity (E) is generated from the relationship between the charge on the particle (q) and the magnitude of the force (F_E) shown in Eqs. (2.36), where q is the charger on the particle which can be estimated by multiplying between an elementary unit of charge (n) in electric field and the elementary unit of charge (e) ($1.6 \times 10^{-19} \text{ C}$), while q is calculated in Eqs. (2.37). The force on a particle with n elementary units of charge in an electric field E is calculated from Eqs. (2.38). In

case of one a single point charge, the electric field can be estimated by placing an imaginary charge (q') in the field and calculated from Eqs. (2.39) (Hinds 1999).

When placed a charged particle in an electric field, it has the particle velocity, which can be determined as the terminal settling velocity. Considering the particle motion in the Stokes region, the terminal electrostatic velocity (V_{TE}) can be estimated from the electrostatic force to Stokes drag as shown in Eqs. (2.40) and (2.41) where B is the particle mechanical mobility. The particle's electrical mobility (Z) is a variable that has the ability of a particle to move in an electric field. It can be calculated from Eqs. (2.42) (Hinds 1999).

$$F_E = K_E \frac{qq'}{R^2} \quad (2.33)$$

$$K_E = \frac{1}{4\pi\epsilon_0} = 9.0 \times 10^9 \text{ N.m}^2/\text{C}^2 \quad (2.34)$$

$$F_E = 9.0 \times 10^9 \frac{qq'}{R^2} \quad (2.35)$$

$$E = \frac{F_E}{q} \quad (2.36)$$

$$q = ne \quad (2.37)$$

$$F_E = qE = neE \quad (2.38)$$

$$E = \frac{F_E}{q'} = \frac{K_E q}{R^2} \quad (2.39)$$

$$neE = \frac{3\pi\eta Vd}{C_c} \quad (2.40)$$

$$V_{TE} = \frac{neEC_c}{3\pi\eta d} = neEB \quad (2.41)$$

$$Z = \frac{V_{TE}}{E} = \frac{neC_c}{3\pi\eta d} = qB = neB, \text{ Re} < 1 \quad (2.42)$$

2.4 Particle Charging

Charging is a process by which aerosol particles acquire charge from flame charging, static electrification, diffusion charging, and field charging. Field and diffusion chargers require high concentrations of unipolar ions, usually by corona discharge. Due to the mutual repulsion and high mobility of these ions, their lifetime are brief. It needs for continuously produced an ion. Ions can be produced by ratio-active discharge, ultraviolet radiation, flames, and corona discharge. The corona discharge can produce unipolar ions at a high concentration of aerosol. To produce a corona discharge, one must establish a nonuniform electrostatic field, such as that between a needle and a plate or between a concentric wire and a tube. Important one is controlling under electric breakdown condition (Intra and Tippayawong 2009; Willeke and Baron 1993).

2.4.1 Diffusion Charging. In case of no electric field, the particle can be charged by diffusion charging. The ions are moved by Brownian random motion to particle, as shown in Figure 2.11. When aerosol particles pass to the gas ions then the ions are colliding to particle and have an electrical charging mechanism of particle. The number of charge ($n_{d(t)}$) on the particle is dependent on particle size, ion density, and time that particles float in the ions or charging time. Eqs. (2.43) is popular and reference in a particle books for calculating the number of charges the diffusion charging, where d_p is the particle diameter (m), k is Boltzmann's constant (1.38×10^{-23}), T is the absolute temperature (Kelvin), K_E is a constant of proportionality ($9.0 \times 10^9 \text{ N.m}^2/\text{C}^2$), e is the elementary unit of charge (1.6×10^{-19} Coulomb), \bar{c}_i is the mean thermal speed of the ions (240 m/s), N_i is the ion concentration (ion/m^3), and t is charging time (s). At standard condition, $N_i t > 10^{12}$ ($\text{ion.s}/\text{m}^3$) for $0.07 < d_p < 1.5 \text{ }\mu\text{m}$ and $N_i t > 10^{13}$ ($\text{ion.s}/\text{m}^3$) for $0.05 < d_p < 40 \text{ }\mu\text{m}$). (Hinds 1999; Intra *et al.* 2016; Willeke and Baron 1993).

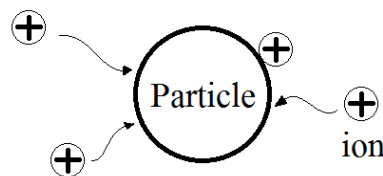


Figure 2.11 Diffusion charging.

2.4.2 Field Charging. Field charging is done by unipolar ions in the region of a high concentration electric field. This charging process shown in Figure 2.12 has a negative and positive electrode in the left and right hand side, respectively. From Figure 2.12 (a), when an uncharged spherical particle is placed in a uniform electric field, it distorts the field. The field lines represent the ion trajectories. The extent of the distortion of the field line depends on the dielectric constant or the relative permittivity (ϵ) of the particle material and charge on the particle (see more in equilibrium charge distribution). Figure 2.12 (b) shows some ion charged into the particle, the field line from negative electrode is less than the positive electrode. When the end of charging process, it has no the field lines from the negative electrode. While both particle and negative electrode have the field line to the positive electrode as shown in Figure 2.12 (c), this condition called the saturation charge (n_s) which can be calculated from Eqs. (2.44) where, and E is electric field (V/m), The field charging can calculate the number of charge ($n_{f(t)}$) by applying the saturation charge equation as shown in Eqs. (2.45) where Z_i is the electrical mobility of ion, it has 1.15×10^{-4} ($\text{m}^2/\text{V s}$) for positive ion and 1.425×10^{-4} ($\text{m}^2/\text{V s}$) for negative ion, which the value of ion properties used by various research. (Hinds 1999; Intra *et al.* 2016; Reischl *et al.* 1996).

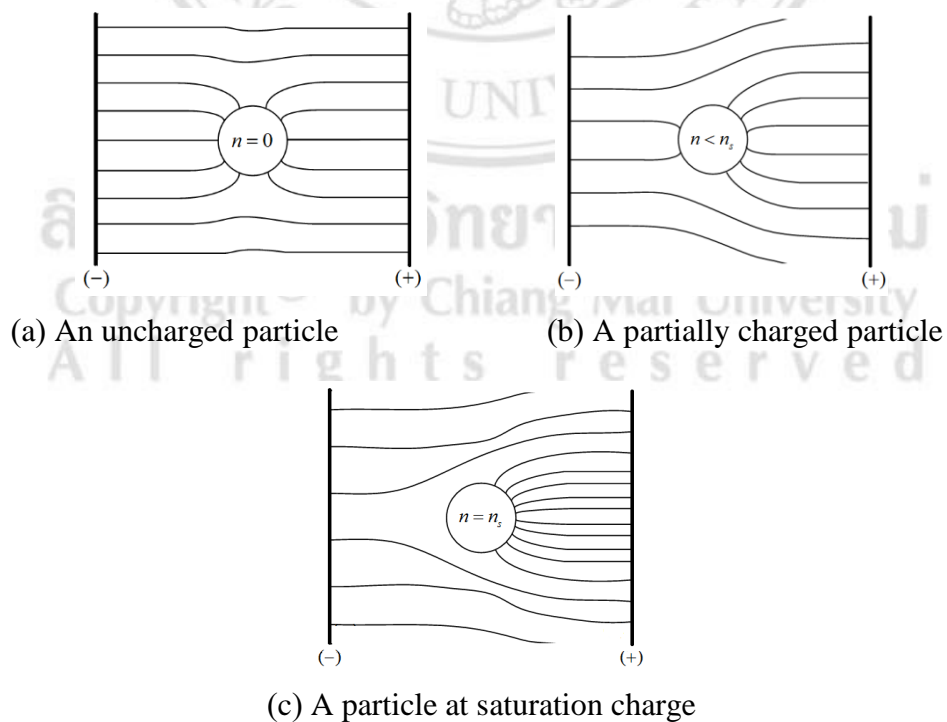


Figure 2.12 Electric field line in the uniform electric field (Hinds 1999).

$$n_{d(t)} = \frac{d_p kT}{2K_E e^2} \ln \left(1 + \frac{\pi K_E d_p \bar{c}_i e^2 N_i t}{2kT} \right) \quad (2.43)$$

$$n_s = \left(\frac{3\varepsilon}{\varepsilon + 2} \right) \left(\frac{Ed_p^2}{4K_E e} \right) \quad (2.44)$$

$$n_{f(t)} = \left(\frac{3\varepsilon}{\varepsilon + 2} \right) \left(\frac{Ed_p^2}{4K_E e} \right) \left(\frac{\pi K_E e Z_i N_i t}{1 + \pi K_E e Z_i N_i t} \right) \quad (2.45)$$

$$n_{c(t)} = n_{d(t)} + n_{f(t)} \quad (2.46)$$

2.4.3 Combined Charging. If ions are generated from corona discharge in nonuniform electric field such as between needle to plate or wire in the cylinder, when particles pass into the corona discharge zone, they are charged by diffusion and field charging or combined charging. The ion number concentration can be found from both charger or combined chargers as shown in Eqs. (2.46), where $n_{d(t)}$ and $n_{f(t)}$ are the number of charges of particle from diffusion and field charging respectively. This diffusion charging has high effect for particles less than 0.2 μm (Hinds 1999; Intra *et al.* 2016; Liu and Kapadia 1978).

2.4.4 Corona Discharge. Air and other gases are normally very good insulators, but they become conductive in a region of sufficient high field strength and have an electrical breakdown between electrical potential. A nonuniform electrostatic field that generated from between a concentric wire and a tube as shown in Figure 2.13 can produce a corona discharge. This corona discharge produces in a thin layer at the surface of the wire. The field strength required for breakdown depends on the wire diameter d_w (m) and is given by the empirical equation from White (1963). A wire 1 mm in diameter as shown in Figure 2.13 put in the tube with a diameter of 0.2 m has a region 0.8 mm thick around the wire exceeds 7,000 kV/m and is the corona discharge region. In the corona region, electrons are accelerated to a velocity sufficient to knock an electron from air molecule upon collision and thereby create a positive ion and a free electron. Within the corona region, this process takes place in a self-sustaining avalanche that produces a dense cloud of a free electrons and positive ions around the wire called corona discharge. The process

is initiated by electrons and ions created by natural radiation. In case of positive wire, the electrons will move rapidly to the wire, and the positive ions will stream away from the wire to the tube in a unipolar “ion wind”. In case of negative wire, the positive ion will go to it, and the electrons will be repelled toward the tube. As their velocity slows with the decreasing field strength at greater distances from the wire, the electrons collide to air molecules forming negative ions, with streams across to the tube. Both positive and negative, ions migrate from the wire to the tube in high concentration of $10^{12} - 10^{15}$ ion/m³ and at high velocities of about 75 m/s. Positive corona, the entire region around the wire has a stable, glowing sheath with a characteristic bluish-green color, while negative corona, the corona glow exists in tufts or brushes that appear to be in a dancing motion over the surface of the wire. A negative corona produces about 10 times as much ozone as a positive corona. The aerosol particles into the space between the concentric wire and the tube will result in field charging of the particles to the same polarity as the wire. The field used to create the corona and the ion wind also causes the field charging. If clean air is blown through the tube at high velocity, it will carry the unipolar ions out of the field region, where they may be mixed with aerosol particles for diffusion charging (Hinds 1999).

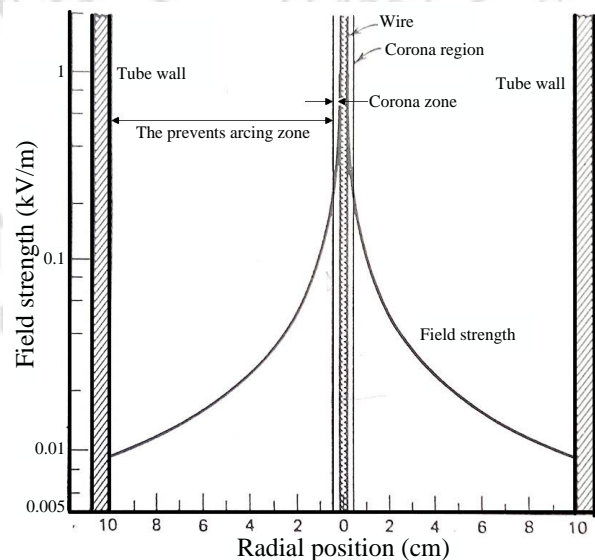


Figure 2.13 Field strength in a tube of diameter 0.2 m with a concentric wire 1 mm in diameter at 50 kV (Hinds 1999).

2.4.5 Charge Limit. There is a fundamental limit of the maximum value in charge that can be acquired by an aerosol particle of a given size. For the negative ion, the maximum charge is reached when the self-generated field at the surface of a particle reaches the value required for spontaneous emission of electrons from a surface. The limitation of the spherical particle is shown in Eqs. (2.47) where E_L is the surface field strength required for spontaneous emission of electron (9.0×10^8 V/m for negative ion and 2.1×10^{10} V/m for positive ion). One's different type limit call Rayleigh limit, it is the controlling limit for most water droplets, because it will be reached before the surface emission limits. This limit can be calculated from Eqs. (2.48) where γ is the surface tension of the droplet liquid ($\gamma = 0.073$ N/m) (Hinds 1999).

$$n_L = \frac{d_p^2 E_L}{4K_E e} \quad (2.47)$$

$$n_L = \left(\frac{2\pi\gamma d_p^3}{K_E e^2} \right)^{1/2} \quad (2.48)$$

Figure 2.14 shows the number of elementary charges from the diffusion, field, combine charging, saturation charge, charging limit, and Rayleigh limit from Eqs. (2.43) to (2.48), respectively. There was considering at 0.01 to 10 μm in diameter at 500 kV/m of electric field, 10^{13} ion./ m^3 of the ion concentration, 2.6 of the relative permittivity, and at standard condition or Normal Temperature and Pressure (NTP). This curve shows that the ion number of the field and diffusion charging are a ratio of d_p^2 and d_p , respectively. The diffusion charging has the effect of the particle that less than about 0.3 μm in diameter. In addition, the positive charge limit has higher than the negative charge limit, which is one reason for selecting a positive charge type. Table 2.2 shows the number of elementary charges from several charging type. Figure 2.15 shows the effect of the electric field strength of the only field charging. The number of elementary charges is set an important variable in the equation from 2.6 of the relative permittivity and 10^{13} ion./ m^3 of the ion concentration. This electric field strength has a high effect to the number of elementary charges significantly. In addition, the number of elementary charges until depends on the dielectric constant from any materials as shown in Figure 2.16. While, the residence time that is important variable in the diffusion and field

charging, it has high effect of the particle less than 1 μm or for the diffusion charging as shown in Figure 2.17. One important variable to be validated is a temperature, this variable has the diffusion charging only. When the temperature is varied between 20 $^{\circ}\text{C}$ to 50 $^{\circ}\text{C}$, it was found that there are very few changes of the number of elementary charges as shown in Figure 2.18. The last of an interest variable is the ion concentration changes in both diffusion and field charging, Figure 2.19 shows that the number of elementary charge has more difference in the diffusion of the particle less than 0.2 μm and the ion concentration that more than 10^{13} ion/m^3 has same result in the field charging (Hinds 1999).

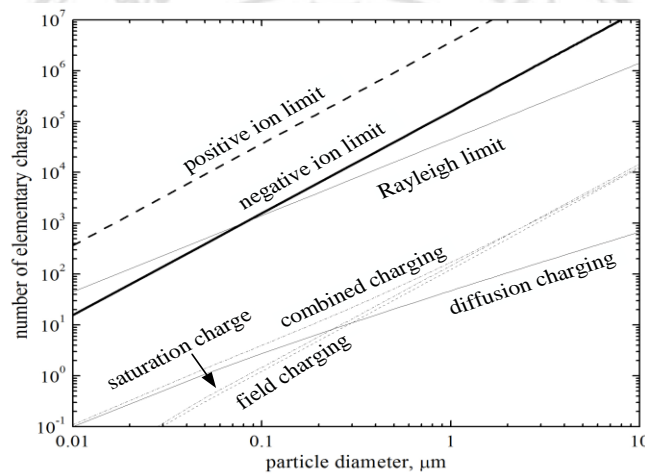


Figure 2.14 The number of elementary charges of the charge limits and the diffusion, field and combine charging.

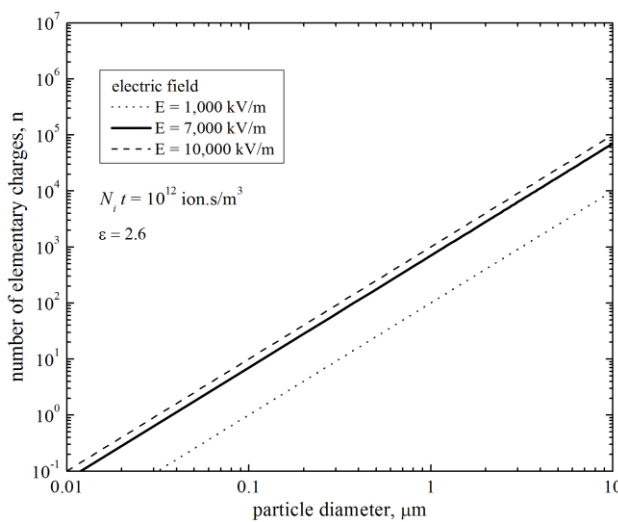


Figure 2.15 Number of elementary charges where the electric field changes.

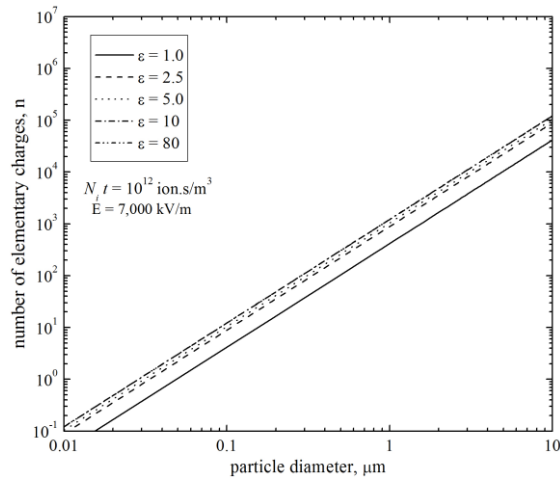


Figure 2.16 Number of elementary charges where the relative permittivity changes.

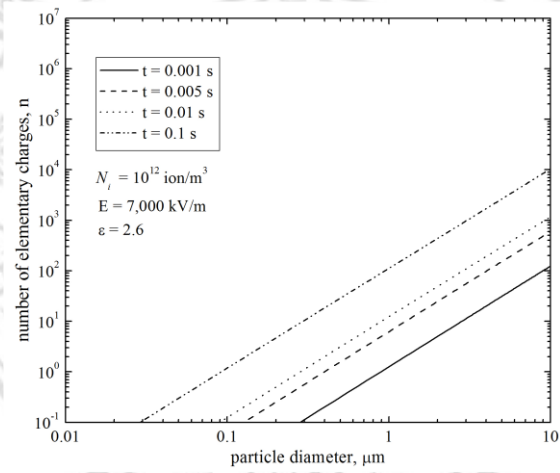


Figure 2.17 Number of elementary charges where the residence time changes.

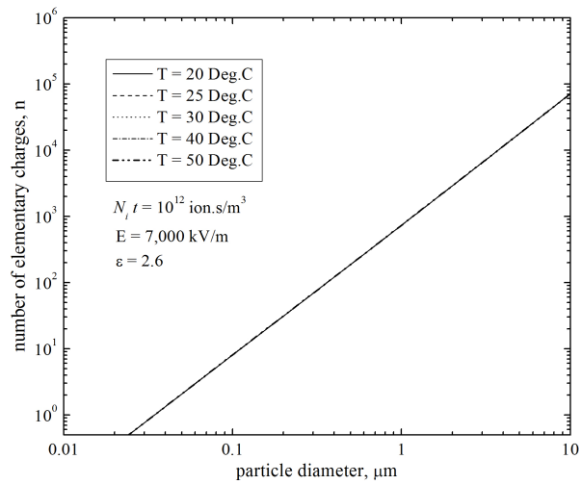


Figure 2.18 Number of elementary charges where the temperature changes.

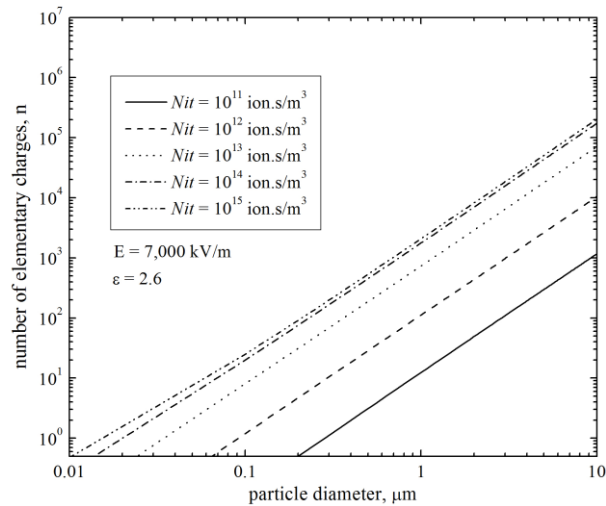


Figure 2.19 Number of elementary charges where the ion concentration changes.

2.5 Filter and Deposition Mechanisms

Fibrous and porous filters are popular for aerosol sampling. Fibrous filters consist of a mat of fine fibers arranged, so it is perpendicular to the direction of airflow. The fibrous filters are usually made from cellulose fibers (wood fibers), glass fibers, or plastic fibers, which have a size range between sub micrometers to 100 μm. Porous membrane filters are made from cellulose esters, sintered metals, polyvinyl chloride, Teflon™, and other plastics. They have different structure from the fibrous filters and have less porosity about 50 to 90%. The particles get out from the gas stream and deposited in the pores. These membrane filters have high efficiency, but a greater resistance to air flow causing for pressure drop more than other filter types. The efficiency for particles smaller than the pore size is not as good as that of porous membrane filters. The fibrous membrane filter is used in industrial air cleaning for high efficiency filtration at high dust concentrations. These filters have a low initial collection efficiency, but becomes high when a dust layer builds up on the fabric.

The efficiency that a fiber can remove particles from aerosol stream is defined in terms of a single-fiber efficiency (E_{γ}). It is the fraction of particles approaching the fiber in the region defined by the projected area of the fiber that are ultimately collected on the fiber as shown in Figure 2.20. E_{γ} is the ratio of the number collected on unit length and the number geometrically incident on unit length. There are five basic mechanisms that an aerosol particle can be deposited onto a fiber filter including interception, inertial

Table 2.2 Comparison of calculation methods for charging by Diffusion, Field, and Combined Charging

at $N_i t = 10^{12}$ ion.s/m³, $\epsilon = 2.6$, NTP.

Particle diameter (μm)	Number of Elementary Units of Charged Acquired; $n_{(t)}$						
	Diffusion Charging	Field Charging	Combine Charging	Saturation Charge	Positive ion limit	Negative ion limit	Rayleigh limit
	Equation (2.43)	Equation (2.45)	Equation (2.46)	Equation (2.44)	Equation (2.47)	Equation (2.47)	Equation (2.48)
0.01	0.02	0.01	0.02	0.01	364	15.63	44.62
0.05	0.32	0.13	0.45	0.37	9,114	390	498
0.1	1.01	0.50	1.51	1.47	36,458	1,562	1,410
0.5	10.81	12.59	23.40	36.80	9.11×10^5	39,062	15,774
1.0	27.31	50.37	77.68	147	3.65×10^6	156,250	44,618
2.5	87.79	314	402	919	2.28×10^7	976,562	176,368
5.0	205	1,259	1,465	3,679	9.11×10^7	3,906,250	4.99×10^5
10.0	471	5,037	5,509	14,719	3.64×10^8	1.56×10^7	1.41×10^6
20.0	1,064	20,148	21,213	58,876	146×10^9	6.25×10^7	3.99×10^6
50.0	3,062	1.26×10^5	1.29×10^5	3.68×10^5	9.11×10^9	3.91×10^8	1.58×10^7
100.0	6,733	5.04×10^5	5.10×10^5	147×10^6	3.65×10^{10}	1.56×10^9	4.46×10^7

ลิขสิทธิ์มหาวิทยาลัยเชียงใหม่
Copyright © by Chiang Mai University
All rights reserved

impaction, diffusion, gravitational settling, and electrostatic attraction. So E_{Σ} can be calculated from Eqs. (2.49) or (2.50) which the efficiency of all types acts independently and is less than one. Interception occurs when particles were flowing with gas streamlines that happens to come within one particle radius of the surface of a fiber, as shown in Figure 2.21. The particle is captured on top (or bottom) of the fiber. The single-fiber efficiency of the interception (E_R) is evaluated from the Kuwabara hydrodynamic factor, the dimensionless parameter from a particle, and a fiber diameter. Inertial impaction of a particle on a fiber occurs when the particle cannot follow quickly with the gas streamline, then it hits the fiber, as show in Figure 2.22. The single fiber efficiency of the inertial impaction (E_I) is evaluated in the same as the interception and still considers Stokes number. The Brownian motion used for validating a small particles, which it has a motion as shown in Figure 2.23. The single-fiber efficiency of the diffusion (E_D) is evaluated by the dimensionless Peclet number. This efficiency increases when the Peclet number and particle size decrease, which is the only deposition mechanism that increases as the particle diameter decreases. In addition, it can be considered an interaction with diffusion, and getting a new form in the single-fiber efficiency of both (E_{DR}). The single-fiber efficiency of the gravitational settling (E_G) is evaluated from the settling velocity, initial velocity, and the dimensionless parameter from a particle and a fiber diameter. The single-fiber efficiency of the electrostatic (E_Q) can be evaluated from the charge on the particle and on fiber, which is difficult to quantify a correct charge. The theory of particle collection of the charged fibers is reviewed by Brown (1993). The collection efficiency of several mechanisms is compared as shown in Figure 2.24. It was found that interception and impaction are negligible for small particle, but increase rapidly for particle larger than $0.3 \mu\text{m}$. While, diffusion is the only important mechanism for particles less than $0.2 \mu\text{m}$. In addition, settling mechanism has a good deposition of particle larger than $5 \mu\text{m}$ (Hinds 1999).

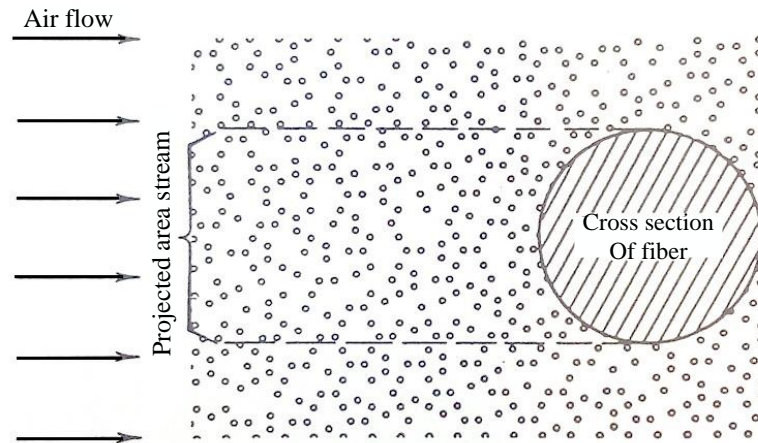


Figure 2.20 Single-fiber efficiency (Hinds 1999).

$$E_{\Sigma} = 1 - (1 - E_R)(1 - E_I)(1 - E_D)(1 - E_{DR})(1 - E_G)(1 - E_q) \quad (2.49)$$

$$E_{\Sigma} \approx E_R + E_I + E_D + E_{DR} + E_G + E_q \quad (2.50)$$

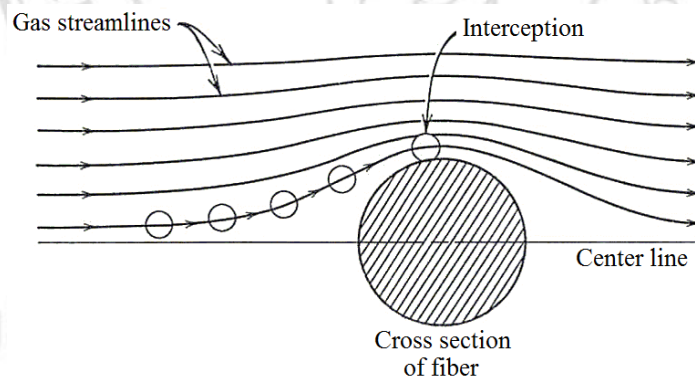


Figure 2.21 Single-fiber collection by interception (Hinds 1999).

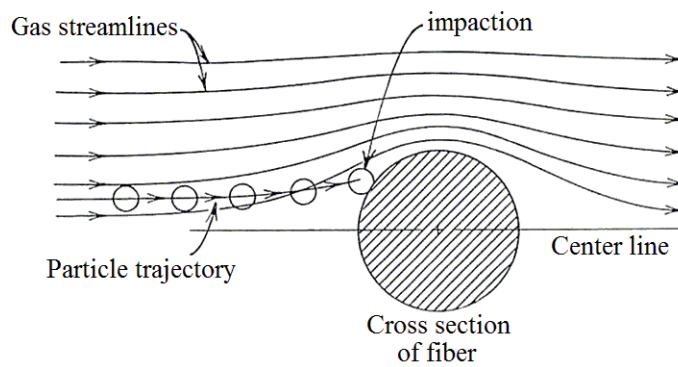


Figure 2.22 Single fiber collection by impaction (Hinds 1999).

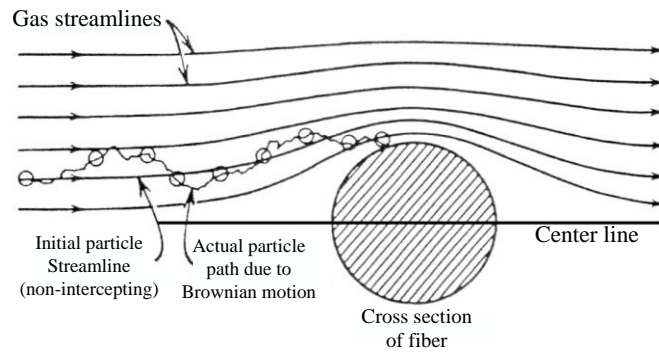


Figure 2.23 Single fiber collection by diffusion (Hinds 1999).

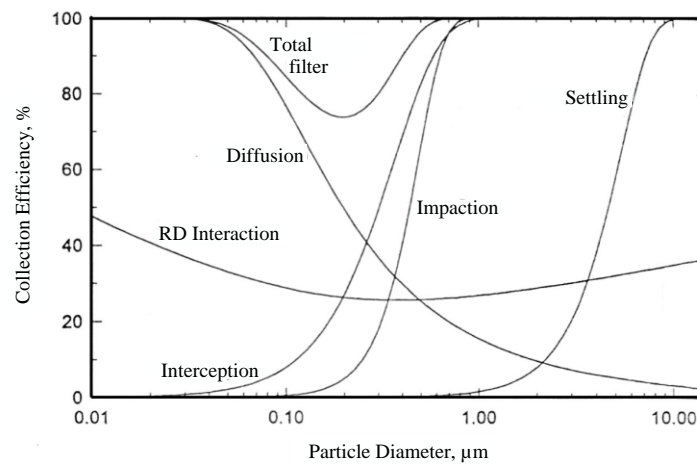


Figure 2.24 The single-fiber efficiency of five basic mechanisms (Hinds 1999).

2.6 Measurement of Flow Rate

Rotameter as shown in Figure 2.25 is a flow meter that has a pressure regulator (needle valve) to maintain a constant flow rate under varying conditions and has scale to indicate a number of flowrate. The regulator maintains a constant pressure drop across the metering valve. It consists of a floating ball free to move up or down in a vertical tapered tube through which the air to be measured passes. The floating ball rises in the tapered tube until its weight balances the upward drag force due to the fluid flowing up through the tube. The area between the floating ball and the tapered tube wall increases as the float rises, reducing the velocity and drag force of the air. The air flow rate (Q) is calculated from Eqs. (2.51), where C_r is a Rotameter coefficient (about 0.6 - 0.8), A_0 is the open area of the tube at the float position, g is the acceleration due to gravity, ρ_g is the gas density, m_f is the float mass and A_f is the cross-sectional area. For operation at difference densities or pressure from standard condition, the flowrate can be calculated

from Eqs. (2.52), where Q_{STP} , ρ_{STP} and p_{STP} are the flow rate, density, and pressure at standard condition, respectively, ρ_r and p_r are the density and pressure at actual condition, respectively (Hinds 1999; Willeke and Baron 1993).

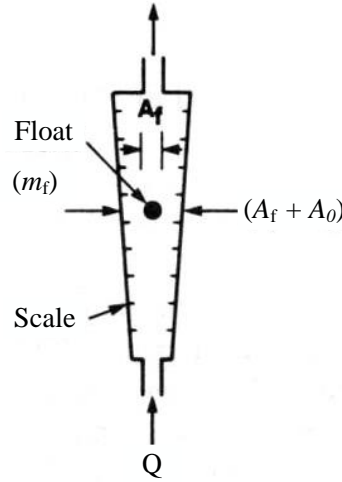


Figure 2.25 Structure of a Rotameter (Willeke and Baron 1993).

$$Q = C_r A_o \left(\frac{2gm_f}{\rho_g A_f} \right)^{1/2} \quad (2.51)$$

$$Q_{STP} = (\text{indicated } Q) \left(\frac{\rho_r}{\rho_{STP}} \right)^{1/2} = (\text{indicated } Q) \left(\frac{P_r}{P_{STP}} \right)^{1/2} \quad (2.52)$$

2.7 Measurement of Ions and Charged Particles

The aerosol electrometer is typically used to measure particles of unipolar charge, which these particles with a net charge concentration of positively or negatively charged particles. The aerosol electrometer shown in Figure 2.26 consists of an electrometer and a filter inside a Faraday cage. It is the simplest form of an electrical aerosol instrument that used in aerosol studies. The charged particles are collected on the filter and generate an electric signal, which is measured by an electrometer (Knutson and Whitby 1975). The Faraday cup method can be used to measure the charge on a wide range of substances and objects such as plastics, films, liquids, gases, and electronic components. A Faraday cup or a Faraday cage is an enclosure made of conductive mesh or sheet metal. The electric field within a close empty conductor is zero and has a cup shield the object placed inside on the support insulator (Tektronix 2016). Faraday cups have several sizes and shape

depending of the object to be tested. Cylindrical and spherical shapes are popular and typically the most convenient. It can be made from simple metal containers like paint cans. The electrodes can be made of any conductive material. The support insulators must be very high resistance such as ceramic or Teflon®. The general connector uses a BNC connector on the outside electrode, but make sure for connecting error may be use welding homogeneous.

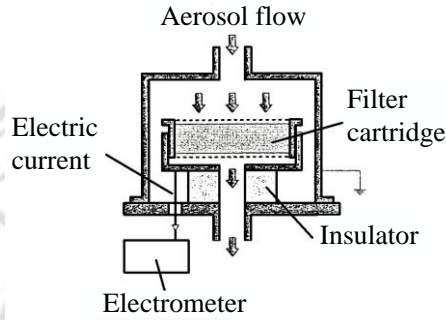


Figure 2.26 Aerosol electrometer (Willeke and Baron 1993).

The electric current (I) is evaluated from Eqs. (2.53) where Q is the sample air flow rate, C_{q+} and C_{q-} are the charge concentrations of positively and negatively, respectively, and C_q is the net charge concentration of the particle. From Gauss' law, the charge collected in the Faraday cup is the induced charge and the filter must not be a conductor. In addition, the current is still dependent on the space-charge density (ρ) or the incoming charged particles and aerosol flow rate (Q_a) as show in Eqs. (2.54) and (2.55) where n_p is the number of particle charge, e is electron charge (1.61×10^{-19} C), N_p is particle number concentration. The current (I_p) from particle is converted to the particle number concentration (N_p) as shown in Eqs. (2.56) where $g(n, d_p)$ is particle probability to get a charge (n_p) of particle diameter (d_p). The particle mass concentration of the measuring particle can be calculated from Eqs. (2.57) (Intra and Tippayawong 2009, 2015; Intra *et al.* 2016; Marjamaki *et al.* 2000; Willeke and Baron 1993).

$$I = (c_q^+ - c_q^-)Q = c_q Q \quad (2.53)$$

$$I_p = \rho Q_a \quad (2.54)$$

$$\rho = n_p e N_p \quad (2.55)$$

$$N_p = \frac{I_p}{g(n_p, d_p) n_p e Q_a} \quad (2.56)$$

$$m_p = \frac{\pi}{6} \frac{I_p}{e Q_a} \int \frac{\rho_p(d_p) d_p^3}{n_p(d_p)} \quad (2.57)$$

An electrometer has a higher sensitivity than a DC multi-meter and can be used to measure ultra-low electric signal. An electrometer is selected to use for the following conditions. (1) Expand a measuring range of a conventional instruments, such as for detecting or measuring currents less than 10 nA (10^{-8} A) and resistances greater than 1G Ω ($10^9 \Omega$). (2) Circuit loading must be minimized, such as when measuring voltage from a source resistance of 100 M Ω or higher and measuring current when input voltage drop of less than a few hundred millivolts is required (when measuring currents from sources of a few volts or less). (3) Charge measurement is required. (4) Measuring signals at or near Johnson noise limitations. Electrometers have four main functions including voltmeter, ammeter, ohmmeter, and coulomb meter (Tektronix 2016). The operating amplifier circuit shown in Figure 2.27 is a basic inverting circuit that popular used for electrometer circuit. Feedback resistor R_f is an amplifier gain which can be calculated from Eqs. (2.58) where I_{in} is the input current and V_{out} is the output voltage (Graskow 2001; He *et al.* 2007; Intra *et al.* 2010, 2012, 2016; Intra and Tippayawong 2008; Intra and Yawootti 2012; Yao *et al.* 2000).

$$R_f = \frac{V_{out}}{I_{in}} \quad (2.58)$$

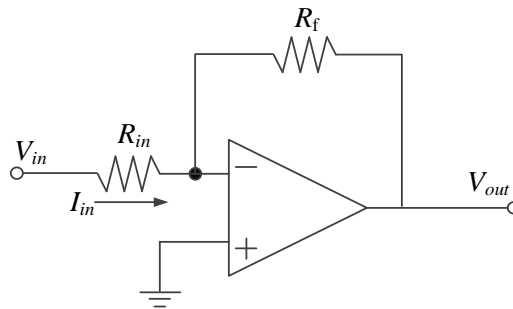


Figure 2.27 Inverting amplifier circuit.

2.8 Data Acquisition

Real time instruments have an analog output signal from the sensor. Most signal is DC voltage about 10V full scale. The old instruments use this analog signal to drive a strip chart recorder. Some instruments use computers to perform data analysis. Personal computer (PC) has high performance for processing a real time analog output. It can adjust depending on user or customer. PC is operated by digital signal based on binary code (0 or 1). It needs for converting an analog input signal to digital for a PC. This function is called analog-to-digital converter or ADC. Digital input of a PC has several types including a parallel port (DB25), a serial port (DB9) such as RS-232, RS-485 and RS-422, USB port, PCMCIA port, and HDMI port. The serial port is one of the popular ports for connecting to an ADC device. Resolution is the ability to distinguish different input signals. ADC will either have a fixed input range that can handle input between 0 - 5 VDC from a general operational amplifier circuit. The resolution of an ADC is usually given in bits number. For example, 8 bit data logger with a working range of 0 - 5 V will break that range into 256 intervals, each interval corresponding to about 0.02 V. The number of intervals (n) is determined by Eqs. (2.59). Resolution (Res) of real time instruments can be calculated from the relation of a full scale of the instrument (FS_M ; $\mu\text{g}/\text{m}^3$), a full scale of ADC (FS_{ADC} ; Volt), a full scale of input from electrometer (FS_I ; Volt), and an interval (n) as shown in Eqs. (2.60). The basic principle for detecting charge on the particle by open-ended Faraday chamber. There are 4 parts of components, including an open-ended Faraday cage, electrometer amplifier, analog to digital converter (ADC), and computer and data processor. The net electric charge ($+q$) on the particle can be measured by accumulating particles in the open-ended Faraday cage. The ultra-low current sensor or electrometer amplifier is used to detect current from electric charge on accumulating particle (about 0 - 2 nA). If the particle charge distribution is a function of particle size (in the form of charge number), then it can find the particle number concentration on the open-ended Faraday cage by Eqs. (2.61), where N_p is particle number concentration (particles/ m^3), I_e is an electrometer current signal (A), η is the ratio of charge particle or charge efficiency (Graskow 2001). The calculation process and processing of computer used binary code that is logic high/low or 0/1 when this signal is a “digital signal”. But signal from electrometer circuit is an analog signal, so it needs to

convert analog to digital signal before sending to computer or processor. The performance of signal convertor is dependent on a resolution which calculated from Eqs. (2.62) where Res is resolution of ADC, V_{iFS} is full scale analog of ADC, n is the most significant bit (MSB) or bit number of ADC. The output digital signal from ADC was connected to computer by input/output port of computer and programming for converting analog input to digital input signal (V_{in}) as shown in Eqs. (2.63) where D is decimal of digital output signal. The analog output is recorded into data logger and sent to graph for analysis with computer (Intra *et al.* 2016).

$$n = 2^{Bits} \quad (2.59)$$

$$Res = \frac{(FS_M) \times (FS_{ADC})}{(FS_I \times n)} \quad (2.60)$$

$$N_p = \frac{I_e}{neQ_a \eta} \quad (2.61)$$

$$Res = \frac{V_{iFS}}{2^n - 1} \quad (2.62)$$

$$V_{in} = \frac{V_{iFS} \times D}{2^n - 1} \quad (2.63)$$

2.9 Comparison with Standards Detectors

US EPA introduces a method to compare the candidate and reference methods in part 53 of Subchapter C, Chapter I by name “Subpart C Procedures for Determining Comparability Between Candidate Methods and Reference Methods” including the general provisions, the test procedure for PM10 and class I method for PM2.5, test procedure for Class II and Class III method for PM2.5 and PM10-2.5 from items 53.30, 53.34 and 53.35, respectively. And Subpart D named “Procedures for Testing Performance Characteristics of Methods for PM10” include the general provisions, the test conditions, generation of test atmospheres for wind tunnel tests, and test procedures from items 53.40, 53.41, 53.42, and 53.43, respectively. Test specifications are defined from Table C4 such as measuring range, minimum number of sites, minimum number of

candidate method samples and reference method samples, minimum number of acceptable sample sets per site under and over $60 \mu\text{g}/\text{m}^3$ mass concentration and minimum number of each season. The testing condition and other details are shown in Table 2.3 (US GPO 2016).

Table 2.3 Testing conditions for PM10 and PM2.5 candidate equivalent methods (US GPO 2016; Judith and John 1998).

Specification	PM10	PM2.5
• Acceptable concentration range (r_j), $\mu\text{g}/\text{m}^3$.	15 – 300	3 – 200
• Minimum number of test sites.	2	1
• Minimum number of candidate method samplers or analyzers per site.	3	3
• Number of reference method samplers per site.	3	3
• Minimum number of acceptable sample sets per site for PM 10 methods:		
○ $r_j < 60 \mu\text{g}/\text{m}^3$	3	-
○ $r_j > 60 \mu\text{g}/\text{m}^3$	3	-
○ Total	10	-
• Minimum number of acceptable sample sets per site for PM 2.5 candidate equivalent methods:		
○ $r_j < 30 \mu\text{g}/\text{m}^3$ for 24-hr or $r_j < 20 \mu\text{g}/\text{m}^3$ for 48-hr samples.	-	3
○ $r_j > 30 \mu\text{g}/\text{m}^3$ for 24-hr or $r_j > 20 \mu\text{g}/\text{m}^3$ for 48-hr samples.	3	-
• Each season	10	23

2.10 Statistical Analysis

2.10.1 Correlation Coefficient. The correlation coefficient is a variable that shows the strength of a linear relationship between comparable data. It is denoted by R that has meaning for interpreting correlation coefficient as shown in Table 2.4. A correlation coefficient of +1 or -1 means a positive or negative correlation, respectively, while 0 is no correlation as shown in Figure 2.28. Pearson's correlation coefficient can be calculated from Eqs. (2.64) or Eqs. (2.65) to (2.70) where x is a first data set, y is a second data set, n is the number of values in each data set, $\sum xy$ is the sum of the data of paired sets, $\sum x$ is the sum of the x data sets, $\sum y$ is the sum of the y data sets, $\sum x^2$ is the sum of the squared x data sets, $\sum y^2$ is the sum of the squared y data sets, $S_{xx,p}$, $S_{xy,p}$ are the auxiliary variable (John *et al.* 1998).

Table 2.4 Meaning of the correlation values (Pearson 2016).

Range	Meaning
$0 \leq R < 0.2$	Very weak correlation
$0.2 < R < 0.4$	Weak correlation
$0.4 < R < 0.6$	Moderate correlation
$0.6 < R < 0.8$	Strong correlation
$0.8 < R \leq 1.0$	Very strong correlation

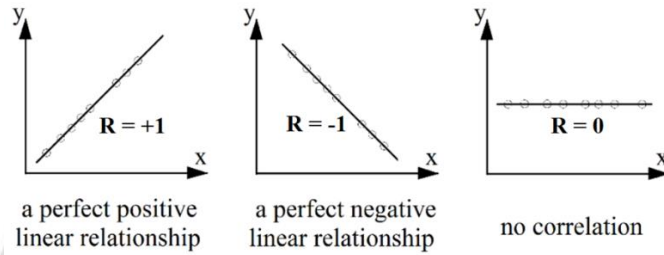


Figure 2.28 Description of the linear relationship (Pearson 2016).

$$R = \frac{\sum xy - \frac{\sum x \sum y}{n}}{\sqrt{\left[\sum x^2 - \frac{(\sum x)^2}{n} \right] \times \left[\sum y^2 - \frac{(\sum y)^2}{n} \right]}} \quad (2.64)$$

$$R = \frac{S_{xy,p}}{\sqrt{S_{xx,p}} \sqrt{S_{yy,p}}} \quad (2.65)$$

$$\overline{\ln x} = \frac{\sum \ln x_i}{n} \quad (2.66)$$

$$\overline{\ln y} = \frac{\sum \ln y_i}{n} \quad (2.67)$$

$$S_{xx,p} = \frac{\sum (\ln x_i - \overline{\ln x})^2}{n} = \frac{\sum \ln x_i^2}{n} - \overline{\ln x}^2 \quad (2.68)$$

$$S_{yy,p} = \frac{\sum (\ln y_i - \overline{\ln y})^2}{n} = \frac{\sum \ln y_i^2}{n} - \overline{\ln y}^2 \quad (2.69)$$

$$S_{xy,p} = \frac{\sum (\ln x_i - \overline{\ln x})(\ln y_i - \overline{\ln y})}{n} = \frac{\sum (\ln x_i \cdot \ln y_i)}{n} - \overline{\ln x} \cdot \overline{\ln y} \quad (2.70)$$

The squared of correlation coefficient (R^2) is the value of variation in x and y data sets that is explained by the linear relationship. Generally it is often called the goodness

of fit. For example, if a correlation coefficient $R = 0.97$ then the coefficient of determination $R^2 = 0.95$, so 95% of the total variation in x and y data sets are described by the linear relationship, but the remaining 5% variation is due to other causes. The relationship between R and R^2 is shown in Figure 2.29.

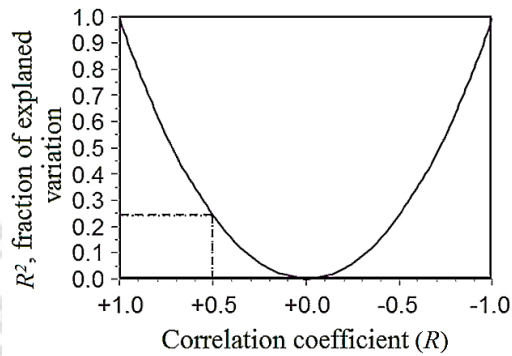


Figure 2.29 Relationship between R and R^2 (Pearson 2016).

2.10.2 Linear Regression Analysis. The linear regression method can fit an equation to a set of x and y data which it yields the best fit for all the data. An approximate fit yields a straight line passed through the set of points in the best possible manner, without being required to pass exactly through any of the points which has a relationship as Eqs. (2.71).

$$y = mx + c \quad (2.71)$$

Generally, the classical linear regression is a function based on $y(x)$ or “ y on x ” which use least square fit for $y(x)$ and it has sum of squares of the y lengths. While the least square fit for $x(y)$ has sum of squares of the x lengths. The orthogonal regression or the major axis line (MAR) minimizes the sum of squares of the lengths and the reduced major axis line (RMA) is regression minimizes the sum of the areas of the triangles as show all in Figure 2.30.

Least squares fit for $y(x)$ and $x(y)$ can be calculated from Eqs. (2.72) and (2.73), respectively. While orthogonal or MAR and RMA can be calculated from Eqs. (2.74) and (2.75), respectively, while other variable is calculated from Eqs. (2.76) to (2.82) where $\gamma = 1$ if $S_{xy} > 0$, $\gamma = 0$ if $S_{xy} = 0$ and $\gamma = -1$ if $S_{xy} < 0$.

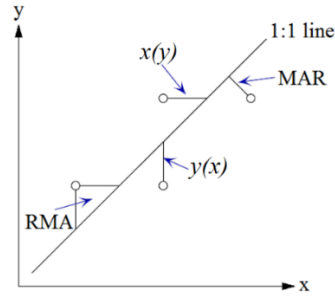


Figure 2.30 Difference of the linear regression (Simfit 2016).

$$y(x) = \beta_1 x + (\bar{y} - \beta_1 \bar{x}) \quad (2.72)$$

$$x(y) = \beta_2 y + (\bar{x} - \beta_2 \bar{y}) \quad (2.73)$$

$$y_1(x) = \beta_3 x + [\bar{y} - \beta_3 \bar{x}] \quad (2.74)$$

$$y_2(x) = \beta_4 x + [\bar{y} - \beta_4 \bar{x}] \quad (2.75)$$

$$\beta_1 = \frac{S_{xy}}{S_{xx}} \quad (2.76)$$

$$\beta_2 = \frac{S_{yy}}{S_{xy}} \quad (2.77)$$

$$\beta_3 = \frac{1}{2} (\beta_2 - (1/\beta_1) + \gamma \sqrt{4 + (\beta_2 - (1/\beta_1))^2}) \quad (2.78)$$

$$\beta_4 = \gamma \sqrt{S_{yy}/S_{xx}} = \gamma \sqrt{\beta_1 \beta_2} \quad (2.79)$$

$$S_{xx} = \frac{1}{(n-1)} \sum_{i=1}^n (x_i - \bar{x})^2 \quad (2.80)$$

$$S_{yy} = \frac{1}{(n-1)} \sum_{i=1}^n (y_i - \bar{y})^2 \quad (2.81)$$

$$S_{xy} = \frac{1}{(n-1)} \sum_{i=1}^n (x_i - \bar{x})(y_i - \bar{y}) \quad (2.82)$$

2.10.3 Power Regression Model. The power regression model is one of nonlinear regression models, which can calculate from Eqs. (2.83) where variables A and B are calculated from Eqs. (2.84) and (2.85).

$$y = Ax^B \quad (2.83)$$

$$B = \frac{S_{xy}}{S_{xx}} \quad (2.84)$$

$$A = e^{\overline{\ln y - B \cdot \overline{\ln x}}} \quad (2.85)$$

2.11 Numerical Modeling of Flow and Electric Field

Mathematical model and numerical simulation may be used to validate an internal flow field, electric field and particle trajectories of the components, including a particle charger, particle size selector and particle detector. COMSOL is a simulation software that can analyze internal flow field, electric field and particle trajectories. 2D modeling is applied in models due to all of the components in a cylindrical coordinate system and symmetry. Numerical modeling for COMSOL is described as follows.

2.11.1 Flow Field Modeling. The fluid flow in this study is assumed to be axisymmetric, laminar, fully developed, and incompressible. Continuity equation and incompressible Navier-Stokes equations are used to calculate this fluid flow. The partial differential equation (PDE) is applied to 2D of the cylindrical coordinate system as shown in Eqs. (2.86) and (2.87) where F is a volume force field such as gravity (N), ρ is the density (kg/m^3), η is the dynamic viscosity ($\text{kg/m}\cdot\text{s}$ or $\text{Pa}\cdot\text{s}$), T is the temperature (Kelvin), p (for flow field modeling) is the pressure (Pa or Pascal), and u is velocity (m/s) which relationship with flow rate and area as shown in Eqs. (2.88) where Q is the air flow rate (m^3/s) and A is an area (m^2). Air density and dynamic viscosity are dependent on RH and temperature. Laboratory for developed and tested the components is located at Doi Saket, Chiang Mai which is 372 m high above sea level. For 0% RH, dynamic viscosity can be calculated from Eqs. (2.89) where η_0 is initial dynamic

viscosity equal 1.8325×10^{-5} (Pa.s). T_0 is the initial temperature equal 296.16 (Kelvin). C is a constant value (120 for 0 % RH) (Tracy *et al.* 1980).

$$F = \rho \frac{\partial u}{\partial t} - \nabla \cdot \left[\eta (\nabla u + (\nabla u)^T) \right] + \rho (u \cdot \nabla) u + \nabla p \quad (2.86)$$

$$\nabla \cdot u = 0 \quad (2.87)$$

$$Q = u \cdot A \quad (2.88)$$

$$\eta = \eta_0 \left[\frac{T_0 + C}{T + C} \left(\frac{T}{T_0} \right)^{1.5} \right] \quad (2.89)$$

2.11.2 Electric Field Modeling. Poisson's equation for the electric potential can be used for electrostatic field modeling. The space-charge effect of the electric field can be neglected ($\rho = 0$) for low aerosol concentration (Chen and Pui 1997; Camata *et al.* 2001). Laplace's equation is shown in Eqs. (2.90) where V is the applied voltage. Current charge, electric potential distribution and electric field distribution are written in Eqs. (2.91) to (2.93) where Q_j is a boundary current source (A/m^2). J is a current density (A/m^2). σ is an electrical conductivity (S/m) (about 5×10^{-15} S/m for electric conductivity of air.). E is an electric field (V/m). J_e is an externally generated current density (A/m^2). For electrostatic equation can be written from Gauss' law by $\rho = 0$ as shown in Eqs. (2.94) where ρ (for electric modeling) is the electric charge density (C/m^3). ϵ_0 is the permittivity of a vacuum has about 8.854×10^{-12} (F/m), ϵ_r is the relative permittivity of material which equal 1 for vacuum and 1.00059 for air.

$$\nabla^2 V = 0 \quad (2.90)$$

$$\nabla \cdot J = Q_j \quad (2.91)$$

$$J = \sigma E + J_e \quad (2.92)$$

$$E = -\nabla V \quad (2.93)$$

$$\rho = -\nabla \cdot (\epsilon_0 \epsilon_r \nabla V) \quad (2.94)$$

2.11.3 Particle Trajectories Modeling. Most particles flow with air flow field, but the impactor in particle size selector component was designed to separate particles from the air flow field. Particles with and without electric charge have different moving forces which needs to know the particle flow for adjustment and increasing the performance. Equations for particle motion involve electrostatic field, Khan and Richardson force, Lagrangian, Hamiltonian, Newtonian, or massless. This thesis used Khan and Richardson equation and electrostatic field for estimating particle trajectories which can be written as Eqs. (2.95) to (2.97) where Re_p is a particle Reynolds number. r_p is the particle radius. ρ (for this model) is the density (kg/m^3). \bar{u} is velocity vector (m/s). \bar{u}_p is the particle velocity vector (m/s). B is the magnetic flux density, v is the velocity (m/s), E is the electric filed (V/m). (COMSOL 2015).

$$F = \pi r_p^2 \rho (\bar{u} - \bar{u}_p)^2 (1.84 (Re_p)^{-0.3} + 0.293 (Re_p)^{0.06})^{3.45} \quad (2.95)$$

$$Re_p = \frac{(|\bar{u} - \bar{u}_p| 2r_p \rho)}{\eta} \quad (2.96)$$

$$F = q(E + v \times B) \quad (2.97)$$

ลิขสิทธิ์มหาวิทยาลัยเชียงใหม่
Copyright© by Chiang Mai University
All rights reserved